Disturbance Observer-Based Sliding Mode Controller for Regulating Pantograph–Catenary Contact Force

Duan, Huayu; Dixon, Roger; Stewart, Edward; Li, Linxiao; Olaby, Osama

DOI:
10.1016/j.ifacol.2023.10.697

Available online at www.sciencedirect.com

ScienceDirect

IFAC PapersOnLine 56-2 (2023) 6069–6074

Disturbance Observer-Based Sliding Mode Controller for Regulating Pantograph–Catenary Contact Force

Huayu Duan, Roger Dixon, Edward Stewart, Linxiao Li, Osama Olaby

Birmingham Centre for Railway Research and Education,
University of Birmingham, Birmingham, United Kingdom
(e-mail: hxd605@student.bham.ac.uk)

Abstract: For most electrified railways, pantographs play a vital role in transmitting energy from overhead line to vehicles, and therefore a stable and continuous contact behavior is required. This paper proposes a disturbance observer-based sliding mode controller (DO-SMC) for the problem of pantograph–catenary contact force regulation. The simulation results show that the DO-SMC with a chattering alleviation approach can effectively reduce contact force fluctuation through a reasonable control input.

Keywords: pantograph and catenary, force regulation, sliding mode control, disturbance observer, active pantograph.

1. INTRODUCTION

Since the pantograph was invented as a type of current collector for the electric locomotive, its advantage in maintaining a stable dynamic contact is preferred for the modern rail transit that is characterized by high speed, reliability, and efficiency. Currently, more than one-third of British railway lines are electrified (Goddard, 2018), and two-thirds of the electrified routes are equipped with overhead lines (also called railway catenary) (Butcher, 2017).

The pantograph–catenary system is presented in Fig. 1, and the pantograph–catenary contact is supposed to be continuous and stable to ensure a healthy energy transmission. However, the natural structure of the catenary system results in an approximately periodical variation in the stiffness of the contact wire, and thus the contact between pantograph and overhead lines forms a coupled oscillation system. With an increase in train operation speed, this system becomes more vulnerable to external interference (Ambrósio et al., 2012). The undesired mechanical interaction and even the loss of contact considerably threaten the train's daily operation (Bucca et al., 2011).

Fig. 1. Pantograph–catenary system

As the pantograph plays such a critical role in the railway, the dynamics of the pantograph–catenary system has been widely studied. Papers have used mathematical models and associated computer programs to analyze the impact of structural designs and operational conditions on the pantograph dynamics. Although it can be seen from simulations that the conventional pantograph has been fitted acceptably in the current operational context (Bruni et al., 2015), its passive mechanism is inherently a potential hazard to the railway due to the lack of robustness and adaptability (Bruni et al., 2018). With the development of the railway industry, researchers started raising concerns about the capability of the current pantograph–catenary system when the running speed increases. Besides that, adapting to the demand for reducing mechanical wear and ensuring high reliability are also required.

As academia and the railway industry paid more attention to pantograph–catenary dynamics, researchers started exploring the possibility of applying active control methods on the pantograph. The most common application of an active controller on the pantograph is regulating the contact force, as the contact force between pantograph and catenary is regarded as a direct indicator related to the quality of the current collection. To realize output feedback, the contact force should be measurable, which can be realized by placing load cells between the collector and its suspension or by fitting fiber optic sensors under the carbon strip (Bruni et al., 2018).

Research on active pantographs can be classified through either the actuator position on the pantograph or the control law. The control force can be applied on the articulated frame, head suspension, or the collectors directly (Bruni et al., 2018). Generally speaking, the control force acting on the lower frame, in a similar way as the pantograph is subjected to the pneumatic force, is the most feasible approach.

Many control methods have been used to make the contact force fluctuation smaller. According to the nominal system, the principle is to reduce the influence of the undesired system variation on the system output. The control laws of the linear quadratic regulator (Ko et al., 2016; Lin et al., 2007; O'Connor et al., 1997; Wu & Brennan, 1997), linear matrix inequality

Peer review under responsibility of International Federation of Automatic Control.
10.1016/j.ifacol.2023.10.697

(Rachid, 2011), and H-infinity (Lu et al., 2017) have been proposed for active pantographs, which demonstrate decent ability in improving the pantograph–catenary dynamics.

As sliding mode control (SMC) has a powerful ability to maintain nominal system dynamics by rejecting disturbances and uncertainties (Edwards & Spurgeon, 1998), an active pantograph based on the SMC was proposed by Pisano and Usai (2008). It was shown that the sliding mode control method can effectively cope with the impact of variations of the catenary model parameters. In recent years, the SMC control scheme is sometimes studied with the disturbance observer (DO) which is an approach to estimating the system disturbance (Sariyildiz et al., 2019). Basically, the DO provides the disturbance information that will be used in the design of the sliding variable and control input. Sliding mode control using a disturbance observer (DO-SMC) has shown a great benefit in attenuating the effect of mismatched disturbances (i.e., the disturbance affects the system via a channel different from the control input) (Ginoya et al., 2013; Yang et al., 2012). Therefore, this paper aims to explore the application of DO-SMC and propose a DO-SMC control law that suits the problem of pantograph–catenary force regulation.

The paper is structured as follows. In section II, the pantograph–catenary model used for controller design and validation will be presented. In section III, the DO-SMC control law for regulating pantograph–catenary contact force will be proposed. In section IV, the control method will be validated with a pantograph–catenary model in simulations. The paper will be concluded in the last section with a discussion.

2. PANTOGRAPH–CATENARY MODELS

Although the pantograph–catenary modelling and simulation benchmark study indicated that the combination of a finite element (FE) catenary and lumped-mass pantograph is a mature method of reproducing the system dynamics (Bruni et al., 2015), the complexity of the FE catenary prevents the application of model-based design methods. Therefore, a linear lumped-mass catenary model is widely used for active controller designs. Integrating the linear catenary with a lumped-mass pantograph, the model is depicted in Fig. 2, and its state-space representation is given as follows, where k_1, k_2, k_3, c_1, c_2, c_3, m_1, m_2, and m_3 are the spring, damper, and mass coefficients of the pantograph; k_4 is the penalty interaction coefficient; m_c, k_c, and c_c are the nominal mass, damper, and stiffness of the catenary; the system states x_1, x_3, x_5 and x_7 denote the mass displacements and x_2, x_4, x_6 and x_8 denote the mass velocities; control input u applies on the pantograph lower frame; and the output y is the pantograph–catenary contact force.

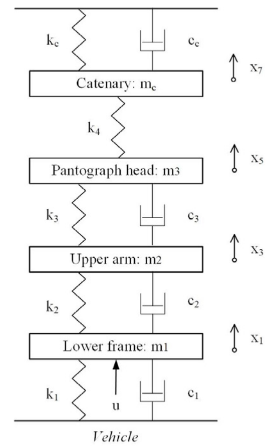

Fig. 2. Linear pantograph–catenary model

$$\dot{x} = Ax + Bu \qquad y = Cx + Du \tag{1}$$

where

$$x = [x_1 \quad x_2 \quad x_3 \quad x_4 \quad x_5 \quad x_6 \quad x_7 \quad x_8]^T$$

$$A = \begin{bmatrix} 0 & 1 & 0 & 0 & 0 & 0 & 0 & 0 \\ -\frac{(k_1+k_2)}{m_1} & -\frac{(c_1+c_2)}{m_1} & \frac{k_2}{m_1} & \frac{c_2}{m_1} & 0 & 0 & 0 & 0 \\ 0 & 0 & 0 & 1 & 0 & 0 & 0 & 0 \\ \frac{k_2}{m_2} & \frac{c_2}{m_2} & -\frac{(k_2+k_3)}{m_2} & -\frac{(c_2+c_3)}{m_2} & \frac{k_3}{m_2} & \frac{c_3}{m_2} & 0 & 0 \\ 0 & 0 & 0 & 0 & 0 & 1 & 0 & 0 \\ 0 & 0 & \frac{k_3}{m_3} & \frac{c_3}{m_3} & -\frac{(k_3+k_4)}{m_3} & -\frac{c_3}{m_3} & \frac{k_4}{m_3} & 0 \\ 0 & 0 & 0 & 0 & 0 & 0 & 0 & 1 \\ 0 & 0 & 0 & 0 & \frac{k_4}{m_c} & 0 & -\frac{(k_4+k_c)}{m_c} & -\frac{c_c}{m_c} \end{bmatrix}$$

$$B = \begin{bmatrix} 0 & \frac{1}{m_1} & 0 & 0 & 0 & 0 & 0 & 0 \end{bmatrix}^T$$

$$C = [0 \quad 0 \quad 0 \quad 0 \quad k_4 \quad 0 \quad -k_4 \quad 0]$$

$$D = 0$$

The parameters of the linear model are summarized in Table 1, where the parameters of the pantograph are obtained from EN 50318:2018 (BSI, 2018) and the parameters of the linear catenary model are estimated through a method proposed in (Duan et al., 2022). The principle of catenary linearization is to make the dynamic behavior of the linear model match the result exhibited in the FE catenary model. As the catenary dynamic behavior varies with train operational conditions, therefore, the linear catenary model is a function of the train speed. In this paper, the train speed of 250 km/h is focused and the parameters of linear catenary model for this speed are obtained as summarised in Table 1.

Table 1. Parameters of the linear model

Parameter	Mass (kg)		Spring constant (N/m)		Damping coefficient (Ns/m)	
Pantograph	m_1	6	k_1	160	c_1	100
	m_2	9	k_2	15500	c_2	0.1
	m_3	7.5	k_3	7000	c_3	45
Interaction	$k_4 = 50000$					
Catenary	m_c	31.72	k_c	2985	c_c	0.695

The controller can be designed based on the linear pantograph–catenary model described above.

To validate active pantograph closed-loop systems, a popular way is using a space (time)-varying stiffness to replace the nominal stiffness k_c of the catenary model to reflect changes in the contact wire property along the train journey. The stiffness look-up table can be obtained from static simulations with an FE catenary model according to Eqn. (2), where F is the static force imposed on the contact wire; and y_{dis} is the static vertical displacement of the measured point. Here, the imposed static force is 115 N, which is in line with the static contact force set for the pantograph in the simulation. The obtained space-varying catenary stiffness is shown in Fig. 3.

$$k_C(x) = \frac{F}{y_{dis}(x)} \tag{2}$$

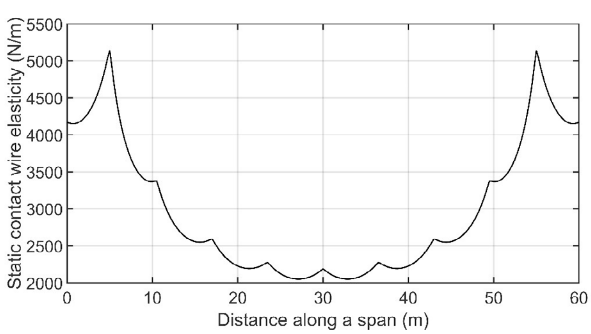

Fig. 3. Space-varying catenary stiffness

3. DISTURBANCE OBSERVER-BASED SLIDING MODE CONTROL

3.1 Problem description

To attenuate the impact of the stiffness variation on the contact force, the control law of the DO-SMC is proposed in this section. The DO assumes that the model is subject to an external disturbance signal, so that the sum of system nonlinearity, parameter perturbation, and external disturbance will be lumped. As shown in Eqn. (3), the system dynamic model is augmented with a disturbance state d, where the matrix E is determined by how the defined disturbance impacts the system. In the pantograph–catenary system, the stiffness variation of the catenary system is defined as the disturbance, which is applied in the form of force (acceleration change) on the mass of the linear catenary model (i.e., $E = [0\ 0\ 0\ 0\ 0\ 0\ 0\ 1]^T$).

$$\begin{aligned} \dot{x} &= Ax + Bu + Ed \\ y &= Cx + Du \end{aligned} \tag{3}$$

3.2 Sliding variable and control law

The SMC belongs to the class of variable structure control. The SMC requires the design of a sliding variable s. Once the states of the system have been found outside the sliding surface $s = 0$, the control input can pull the states back onto the sliding surface in finite time and the nominal system behavior can be maintained (Edwards & Spurgeon, 1998).

The sliding variable is designed as follows with the aim that the output error can approach zero, where g is the gain to be designed and y and y_d are the actual and desired output, respectively. For the following contact force regulation task, y_d is a constant equal to 115.

$$\begin{aligned} s &= ge + \dot{e} \\ e &= y - y_d \end{aligned} \tag{6}$$

Here, a DO-SMC control law for the pantograph–catenary contact force regulation problem is developed. The sliding variable becomes Eqn. (7) by combining (3) and (6), considering the system dynamics depicted in Eqn. (1) that $CB = 0$, $CE = 0$, $D = 0$.

$$s = (gC + CA)x - gy_d \tag{7}$$

The control input is designed below.

$$u = -(CAB)^{-1}[(gCA + CA^2)x + (Dis_{max} + \sigma)sgn(s)] \tag{8}$$

where

$$Dis = |CAEd|$$

Dis_{max} is the upper bound of the disturbance $CAEd$. To ensure the control input can always help the states back to the sliding surface, the reachability condition is proved as follows.

From Eqn. (7),

$$\dot{s} = (gCA + CA^2)x + CABu + CAEd \tag{9}$$

Let control input

$$u = -(CAB)^{-1}[(gCA + CA^2)x + v] \tag{10}$$

Combining Eqns. (9) and (10),

$$\dot{s} = -v + CAEd \tag{11}$$

Let

$$v = (Dis_{max} + \sigma)sgn(s) \tag{12}$$

Then

$$\begin{aligned} s\dot{s} &= -sv + sCAEd \\ s\dot{s} &= -Dis_{max}|s| - \sigma|s| + sCAEd \\ s\dot{s} &\le -\sigma|s| \le 0 \end{aligned} \tag{13}$$

The reachability is proved. The design of control input Eqn. (8) requires the knowledge of d as Dis_{max} needs to be estimated. The disturbance d can be estimated offline from a disturbance observer. One of the conditions of applying this control law is Eqn. (14). If the control force acts on m_3 (pantograph head), the condition can be met.

$$CAB \neq 0 \tag{14}$$

However, if the control input acts on m_1 (the pantograph lower frame, which is the most feasible solution), the condition

Eqn. (14) cannot be met. To apply the SMC in this case, the sliding variable is modified as follows.

$$s = g_1 e + g_2 \dot{e} + g_3 \ddot{e} + \dddot{e}$$
$$= (g_1 C + g_2 CA + g_3 CA^2 + CA^3)x$$
$$+(g_3 CAE + CA^2 E)d + CAE\dot{d} - g_1 y_d \quad (15)$$

The control input is designed as follows.

$$u = -(CA^3B)^{-1}[(g_1CA + g_2CA^2 + g_3CA^3 + CA^4)x$$
$$+(Dis_{max} + \sigma)sgn(s)] \quad (16)$$

where

$$Dis = |(g_2CA + g_3CA^2 + CA^3)Ed|$$
$$+|(g_3CA + CA^2)E\dot{d}| + |CAE\ddot{d}|$$

The reachability proof is omitted as it is similar to the previous case. Dis now consists of the disturbance and its first- and second-order derivatives that need to be estimated. Also, the sliding variable is now a function of d and $\dot{d}$, which requires a DO to estimate the disturbance in real time to synthesize the control input.

The gain $g_i (i = 1,2,3 \cdots)$ in the sliding variable s can be selected through the method proposed by Lin and Hsiao (2020), so that the eigenvalues of the sliding surface $s = 0$ can be located in the left plane that makes the error e approach to zero.

$$s = \left(\frac{d}{dt} + g\right)^n e \quad (17)$$

For example, if $n = 3$ (i.e., the third-order derivative of the error exists), the sliding variable can be rewritten as Eqn. (18), by doing so, only one variable needs to be tuned.

$$s = g^3 e + 3g^2 \dot{e} + 3g\ddot{e} + \dddot{e} \quad (18)$$

3.3 First-order disturbance observer

To estimate the disturbance d and its derivative $\dot{d}$, the first-order DO will be used. For a first-order DO, the system dynamics is augmented with a disturbance state (d) and its derivative, as shown in Eqn. (19) which assumes that $\ddot{d} = 0$. The disturbance states can be then observed through a state observer. The observer gain is supposed to be designed based on the requirement of the bandwidth.

$$\begin{bmatrix} \dot{x} \\ \dot{d} \\ \ddot{d} \end{bmatrix} = \begin{bmatrix} A & E & 0 \\ 0 & 0 & 1 \\ 0 & 0 & 0 \end{bmatrix} \begin{bmatrix} x \\ d \\ \dot{d} \end{bmatrix} + \begin{bmatrix} B \\ 0 \\ 0 \end{bmatrix} u$$
$$y = [C \quad 0 \quad 0] \begin{bmatrix} x \\ d \\ \dot{d} \end{bmatrix} + Du \quad (19)$$

3.4 Chattering alleviation

Alleviation of the chattering problem is often to be considered when applying an SMC. An alleviation method (Ginoya et al., 2013) is applied in this paper, which introduces a linear term in the control input that can make it possible to use a smaller switching gain k_s (i.e., $Dis_{max} + \sigma$).

For the sliding variable containing the third-order derivative of the error, the control input is modified as follows, where k_l is the SMC linear gain and k_s is the SMC switching gain, which are to be designed.

$$u = -(CA^3B)^{-1}[(g_1CA + g_2CA^2 + g_3CA^3 + CA^4)x$$
$$+k_l s + k_s sgn(s)] \quad (20)$$

4. VALIDATION OF ACTIVE PANTOGRAPHS

Based on the nominal linear model and its parameters, the sliding variable and the control input can be designed according to Eqns. (15)–(17), and $g = 50$ is selected to balance the control input and control performance.

If the chattering alleviation method is not applied, k_s is identical to $Dis_{max} + \sigma$, where Dis_{max} is a function of the system disturbance and its first- and second-order derivatives, which can be estimated from a second-order DO offline. The estimated system disturbance Dis is presented in Fig. 4 and $Dis_{max} + \sigma$ is 5.62×10^8. The magnitude of such a large number implies that this control method is sensitive to the estimated disturbance (which will include noise in practice).

The control input can then be designed, which is a function of the observed system and disturbance states.

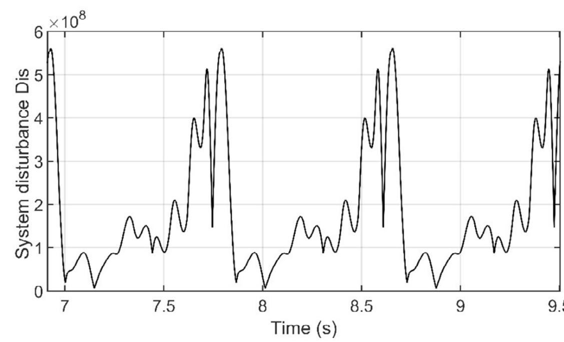

Fig. 4. Disturbance $Dis = |(g_2CA + g_3CA^2 + CA^3)Ed| + |(g_3CA + CA^2)E\dot{d}| + |CAE\ddot{d}|$

The simulation results of the DO-SMC are given below, where Fig. 5 shows the control input and Fig. 6 presents the output (i.e., contact force). It can be seen that the DO-SMC-based active pantograph can effectively reduce the contact force fluctuation, but besides the chattering phenomenon, the magnitude of control input is also unacceptable. This is mainly because the controller needs much extra efforts to dynamically cancel out the mismatched disturbance through the control input channel.

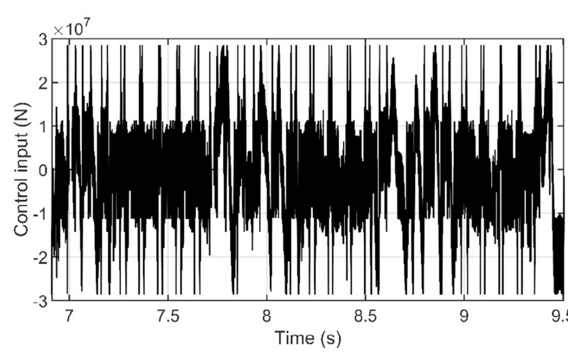

Fig. 5. Control input (no chattering alleviation)

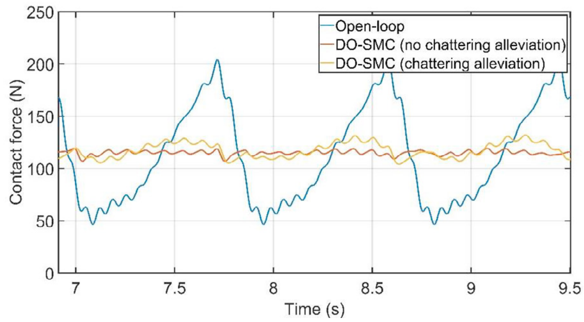

Fig. 6. System output contact force

When the chattering alleviation method is adopted, the linear gain k_l is chosen as 100 and the switching gain k_s is reduced to 1×10^4. The contact force result is shown and compared with the open-loop and no-chattering-alleviation cases in Fig. 6. Although the disturbance rejection performance decreases slightly compared to the no-chattering-alleviation method, its effectiveness remains evident. However, as shown in Fig. 7, there is a significant reduction in control input. The minimum control input is above zero, which means the actuators only need to produce control input in one direction.

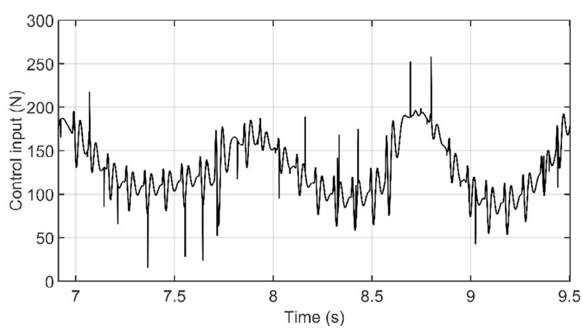

Fig. 7. Control input (with chattering alleviation)

The numerical results of the control performance are summarised in Table 2. The minimum (*min*), maximum (*max*) and standard deviation (*std*) values of the control input and output are compared. It is shown that the proposed DO-SMC control law is able to significantly reduce the variation of the contact force. With the chattering alleviation method, the unrealistic control input can be mitigated to a reasonable level.

Table 2. Numerical results of the DO-SMC pantograph

Indicator	*Control input*			*Control output (contact force)*		
	min	*max*	*std*	*min*	*max*	*std*
Passive pantograph	Not Applicable			46.52	204.10	46.36
DO-SMC (without alleviation)	-2.86×10^7	2.86×10^7	1.11×10^7	107.07	119.34	2.19
DO-SMC (with alleviation)	15.43	258.04	33.14	104.10	132.14	7.27

5. DISCUSSION AND CONCLUSIONS

This paper proposes a DO-SMC for the contact force regulation problem of the pantograph–catenary system. The source of the pantograph–catenary contact force fluctuation is lumped as an external disturbance. To attenuate the influence of such mismatched disturbance, an SMC is proposed, aiming to eliminate the output error. As the controller needs information of the states of the disturbance and its derivative, a first-order DO is integrated with the SMC. The simulations show that the DO-SMC has significant effectiveness in attenuating the influence of disturbance. However, the standard DO-SMC law results in an unacceptable control input regarding the magnitude and chattering phenomenon. When chattering alleviation is adopted, the control input becomes reasonable and the control performance in reducing contact force fluctuation remains good.

As the control law contains the derivative of the disturbance, this closed-loop system is sensitive to high-frequency change (disturbance) over the nominal model. This feature is critical and requires further study because, when the time-varying stiffness is used as the source of the system perturbation (as in this paper), only the low-frequency components in the disturbance can be represented (Duan et al., 2022). Therefore, more refined catenary models need to be used to validate the proposed DO-SMC control scheme. From a practical point of view, the dynamics of the input actuator and the noise of the measurement also need to be considered in the closed loop. Furthermore, it is worthwhile to compare the proposed control method with other control laws regarding the control efficiency.

ACKNOWLEDGMENT

This work was financially supported by the School of Engineering, University of Birmingham and China Scholarship Council under Grant No. 201908060338.

REFERENCES

Ambrósio, J., Pombo, J., Pereira, M., Antunes, P., & Mósca, A. (2012). A computational procedure for the dynamic analysis of the catenary-pantograph interaction in high-speed trains. *Journal of Theoretical and Applied Mechanics*, *50*(3), 681-699.

Bruni, S., Ambrosio, J., Carnicero, A., Cho, Y. H., Finner, L., Ikeda, M., . . . Zhang, W. (2015). The results of the pantograph–catenary interaction benchmark. *Vehicle System Dynamics*, *53*(3), 412-435.

Bruni, S., Bucca, G., Carnevale, M., Collina, A., & Facchinetti, A. (2018). Pantograph–catenary interaction: recent achievements and future research challenges. *International Journal of Rail Transportation*, *6*(2), 57-82.

BSI. (2018). EN 50318:2018 Railway applications — Current collection systems — Validation of simulation of the dynamic interaction between pantograph and overhead contact line. London: British Standards Institution.

Bucca, G., Collina, A., Manigrasso, R., Mapelli, F., & Tarsitano, D. (2011). Analysis of electrical interferences related to the current collection quality in pantograph–catenary interaction. *Proceedings of the Institution of Mechanical Engineers, Part F: Journal of Rail and Rapid Transit*, *225*(5), 483-500.

Butcher, L. (2017). *Rail Electrification*. House of Commons Library Briefing Paper no. SN05907. London: House of Commons Library.

Duan, H., Dixon, R., & Stewart, E. (2022). A disturbance observer based lumped-mass catenary model for active pantograph design and validation. *Vehicle System Dynamics*, 1-18.

Edwards, C., & Spurgeon, S. (1998). *Sliding Mode Control: Theory and Applications*. Boca Raton, FL: CRC Press.

Ginoya, D., Shendge, P., & Phadke, S. (2013). Sliding mode control for mismatched uncertain systems using an extended disturbance observer. *IEEE Transactions on Industrial Electronics*, *61*(4), 1983-1992.

Goddard, A. (2018). *Rail Infrastructure, Assets and Environmental*. London: Office of Rail and Road.

Ko, M. T., Yokoyama, M., Yamashita, Y., Kobayashi, S., & Usuda, T. (2016). Contact force control of an active pantograph for high speed trains. *Journal of Physics: Conference Series*, *744*(1), 012151.

Lin, C.-H., & Hsiao, F.-Y. (2020). Proportional-integral sliding mode control with an application in the balance control of a two-wheel vehicle system. *Applied Sciences*, *10*(15), 5087.

Lin, Y. C., Lin, C. L., & Yang, C. C. (2007). Robust active vibration control for rail vehicle pantograph. *IEEE Transactions on Vehicular Technology*, *56*(4 II), 1994-2004.

Lu, X., Liu, Z., Zhang, J., Wang, H., Song, Y., & Duan, F. (2017). Prior-information-based finite-frequency H infinity control for active double pantograph in high-speed railway. *IEEE Transactions on Vehicular Technology*, *66*(10), 8723-8733.

O'Connor, D. N., Eppinger, S. D., Seering, W. P., & Wormley, D. N. (1997). Active control of a high-speed pantograph. *Journal of Dynamic Systems, Measurement, and Control*, *119*(1), 1-4.

Pisano, A., & Usai, E. (2008). Contact force regulation in wire-actuated pantographs via variable structure control and frequency-domain techniques. *International Journal of Control*, *81*(11), 1747-1762.

Rachid, A. (2011). Pantograph catenary control and observation using the LMI approach. *2011 50th IEEE Conference on Decision and Control and European Control Conference*, 12-15 Dec. 2011, pp. 2287-2292.

Sariyildiz, E., Oboe, R., & Ohnishi, K. (2019). Disturbance observer-based robust control and its applications: 35th anniversary overview. *IEEE Transactions on Industrial Electronics*, *67*(3), 2042-2053.

Wu, T. X., & Brennan, M. J. (1997). Active vibration control of a railway pantograph. *Proceedings of the Institution of Mechanical Engineers, Part F: Journal of Rail and Rapid Transit*, *211*(2), 117-130.

Yang, J., Li, S., & Yu, X. (2012). Sliding-mode control for systems with mismatched uncertainties via a disturbance observer. *IEEE Transactions on Industrial Electronics*, *60*(1), 160-169.